

## Asymmetric unimodal maps at the edge of chaos

Ugur Tirnakli,<sup>1,\*</sup> Constantino Tsallis,<sup>2,†</sup> and Marcelo L. Lyra<sup>3,‡</sup>

<sup>1</sup>Department of Physics, Faculty of Science, Ege University, 35100 Izmir, Turkey

<sup>2</sup>Centro Brasileiro de Pesquisas Físicas, Rua Xavier Sigaud 150, 22290-180 Rio de Janeiro, RJ, Brazil

<sup>3</sup>Departamento de Física, Universidade Federal de Alagoas, 57072-970 Maceió, AL, Brazil

(Received 18 September 2001; published 11 February 2002)

We numerically investigate the sensitivity to initial conditions of asymmetric unimodal maps  $x_{t+1} = 1 - a|x_t|^{z_i}$  ( $i=1,2$  correspond to  $x_t > 0$  and  $x_t < 0$ , respectively,  $z_i > 1$ ,  $0 < a \leq 2$ ,  $t=0,1,2,\dots$ ) at the edge of chaos. We employ three distinct algorithms to characterize the power-law sensitivity to initial conditions at the edge of chaos, namely: direct measure of the divergence of initially nearby trajectories, the computation of the rate of increase of generalized nonextensive entropies  $S_q$ , and multifractal analysis. The first two methods provide consistent estimates for the exponent governing the power-law sensitivity. In addition to this, we verify that the multifractal analysis does not provide precise estimates of the singularity spectrum  $f(\alpha)$ , especially near its extremal points. Such feature prevents to perform a fine check of the accuracy of the scaling relation between  $f(\alpha)$  and the entropic index  $q$ , thus restricting the applicability of the multifractal analysis for studying the sensitivity to initial conditions in this class of asymmetric maps.

DOI: 10.1103/PhysRevE.65.036207

PACS number(s): 05.45.-a, 05.20.-y, 05.70.Ce

### I. INTRODUCTION

In recent years, there has been an increasing interest in the behavior of the one-dimensional dissipative maps at their chaos threshold [1–9]. When the sensitivity to the initial conditions is examined at the onset of chaos, the sensitivity function, defined through

$$\xi(t) = \lim_{\Delta x(0) \rightarrow 0} \frac{\Delta x(t)}{\Delta x(0)}, \quad (1)$$

[where  $\Delta x(0)$  and  $\Delta x(t)$  are the discrepancies of the initial conditions at times 0 and  $t$ ], can be put in a conveniently generalized form

$$\xi(t) = [1 + (1 - q)\lambda_q t]^{1/(1-q)} \quad (q \in \mathcal{R}), \quad (2)$$

(solution of  $\dot{\xi} = \lambda_q \xi^q$ ) where  $\lambda_q$  is the generalized Lyapunov exponent. This equation recovers the standard exponential form  $\exp(\lambda_1 t)$  for  $q=1$  (here,  $\lambda_1$  is the standard Lyapunov exponent), but generically  $q \neq 1$  corresponds to a power-law behavior. In this case, if  $\lambda_q < 0$  and  $q > 1$  ( $\lambda_q > 0$  and  $q < 1$ ) the system is said to be *weakly* insensitive (sensitive) to the initial conditions, a situation that is different from the standard case where we have *strong* insensitivity (sensitivity) for  $\lambda_1 < 0$  ( $\lambda_1 > 0$ ).

Although asymptotic power-law sensitivity to initial conditions was observed previously [10–12],  $\xi(t)$  as given by Eq. (2) provides a more complete description than just  $\xi(t) \propto t^{1/(1-q)}$  ( $t \gg 1$ ), in the sense that it provides not only the exponent but also the coefficient  $\lambda_q$  and moreover it is expected to be correct not only at very large times but also at intermediate times after a possibly quick transient. At the

edge of chaos,  $\xi(t)$  presents strong fluctuations with time, reflecting the fractal structure of the critical attractor, and Eq. (2) delimits the power-law growth of the upper bounds of the sensitivity function. These upper bounds allow us to estimate the proper value  $q^*$  of the index  $q$  for the map under consideration. This method has already been successfully used for a variety of one-dimensional dissipative maps such as logistic [1],  $z$ -logistic [2], circle [3],  $z$ -circular [4] maps.

The second method of estimating the  $q^*$  value of the map under consideration comes from the geometrical aspects of the attractor at the chaos threshold. This method is based on the multifractal singularity spectrum  $f(\alpha)$ , which reflects the fractal dimension of the subset with singularity strength  $\alpha$  [13,14]. The  $f(\alpha)$  function is a downward parabolalike concave curve and typically vanishes at two points, namely,  $\alpha_{min}$  and  $\alpha_{max}$ , characterizing the scaling behavior of the most concentrated and most rarefied regions on the attractor. The study of the scaling behavior of these regions led two of us to propose a scaling relation as [3]

$$\frac{1}{1-q^*} = \frac{1}{\alpha_{min}} - \frac{1}{\alpha_{max}} \quad (q^* < 1). \quad (3)$$

This is, in fact, a fascinating relation since it connects the power-law sensitivity to initial conditions of such dynamical systems with purely geometrical quantities and consequently provides a completely different method for the determination of the proper  $q^*$  value of the map under consideration. This method has also been used so far for logistic [3],  $z$ -logistic [3], circle [3] and  $z$ -circular [4] maps, and the results obtained for the  $q^*$  values are, within a good precision, the same as those of the first method.

In order to make the situation even more enlightening, a third method of obtaining the proper  $q^*$  value of a given map has been introduced very recently using a specific generalization of the Kolmogorov-Sinai (KS) entropy [5,6]. It is known that, for a chaotic dynamical system, the rate of loss

\*Email address: tirnakli@sci.ege.edu.tr

†Email address: tsallis@cbpf.br

‡Email address: marcelo@fis.ufal.br

of information can be characterized by the KS entropy ( $K_1$ ) and it is defined as the increase, per unit time, of the standard Boltzmann-Gibbs entropy  $S_1 = -\sum_{i=1}^W p_i \ln p_i$  (we use  $k_B = 1$ ). In fact, the KS entropy is defined, in principle, through a *single trajectory* in phase space based on the frequencies of appearance, in increasingly long strips, of symbolic sequences of the regions of the partitioned phase space [15]. However, apparently in almost all cases, this definition can be equivalently replaced by an ensemble-based procedure, which is, no doubt, by far simpler computationally than the former procedure. This ensemble-based version is the one we use herein. On the other hand, it is worth noting that a single-trajectory-based procedure has been used very recently in [16].

From the Pesin equality, namely,  $K_1 = \lambda_1$  if  $\lambda_1 > 0$  and  $K_1 = 0$  otherwise, it is evident that the KS entropy is deeply related to the Lyapunov exponents. The KS entropy rate is then defined through  $K_1 \equiv \lim_{t \rightarrow \infty} \lim_{W \rightarrow \infty} \lim_{N \rightarrow \infty} S_1(t)/t$ , where  $t$  is the time,  $W$  is the number of regions in the partition of the phase space and  $N$  is the number of initial conditions (all chosen at  $t=0$  within one region among the  $W$  available ones) that are evolving in time. On the other hand, for the marginal cases where  $\lambda_1 = 0$ , a generalized version of the KS entropy  $K_q$  has been introduced [1] as the increase rate of a proper nonextensive entropic form, namely,

$$S_q(t) = \frac{1 - \sum_{i=1}^W [p_i(t)]^q}{q-1}. \quad (4)$$

This entropy enables a generalization of the standard Boltzmann-Gibbs statistics [17,18] and it covers the BG entropy as a special case in the  $q \rightarrow 1$  limit. A general review and related subjects on this nonextensive formalism can be found in Ref. [19]; recent applications in high-energy physics, turbulence, and biology can be seen in Refs. [20], [21], and [22], respectively. Therefore, for the generalized version of KS entropy, the entropy rate is proposed to be

$$K_q \equiv \lim_{t \rightarrow \infty} \lim_{W \rightarrow \infty} \lim_{N \rightarrow \infty} \frac{S_q(t)}{t}. \quad (5)$$

Consistently, the Pesin equality is also expected to be generalizable as  $K_q = \lambda_q$  if  $\lambda_q > 0$  and  $K_q = 0$  otherwise.

Consequently, these ideas have been used very recently to construct a third method of estimating the  $q^*$  values [5]. It is conjectured that (i) a unique value of  $q^*$  exists such that  $K_q$  is finite for  $q = q^*$ , vanishes for  $q > q^*$ , and diverges for  $q < q^*$ ; (ii) this value of  $q^*$  coincides with that coming from the other two methods described previously. These conjectures have been verified with numerical calculations, at the edge of chaos, for the standard logistic map [5], logisticlike map family, and generalized cosine map [6], which strongly supports the point that all three methods yield one and the same special  $q^*$  value of a map under consideration. At this point, it is worth mentioning that when the initial conditions are very spread in phase space (instead of the localized

ones), another class of  $q^*$  values (above unity instead of below unity) has been found for  $z$ -logistic case [23].

Although these three different methods of finding  $q^*$  value have been already tested and numerically verified for a number of one-dimensional dissipative map families, it is no doubt convenient (in the spirit of further clarifying their domain of validity) to test them in more general grounds. For example, all the maps discussed so far belong to one-dimensional, dissipative, symmetric, one- or two-parameter unimodal families. At this point, one can ask what happens for the (i) two- (or more) dimensional maps, (ii) conservative maps, (iii) asymmetric families. Needless to say, if any one of these cases could be analyzed with the above mentioned three methods consistently, the scenario would obviously become more robust. In the present effort, we shall try to make a step forward addressing the point (iii), namely, the asymmetric three-parameter family of logistic map of the form

$$x_{t+1} = f(x_t) \equiv \begin{cases} 1 - a|x_t|^{z_1} & \text{if } x_t \geq 0, \\ 1 - a|x_t|^{z_2} & \text{if } x_t \leq 0, \end{cases} \quad (6)$$

where  $z_{1,2} > 1$ ,  $0 < a \leq 2$ ,  $-1 \leq x_t \leq 1$  and  $t = 0, 1, 2, \dots$ .

## II. ASYMMETRIC LOGISTIC MAP FAMILY: NUMERICAL RESULTS

The properties of this kind of asymmetric map family have already been studied [24–26]. The asymmetric shape of the map family is illustrated in Fig. 1(a) for a typical value of  $(z_1, z_2)$  pair, whereas in Fig. 1(b) the bifurcation diagram has been plotted. Before the onset of chaos, the sequence of bifurcations is the same as that of Feigenbaum, but in the chaotic region (after the onset of chaos), the relative sizes of the various windows are quite different from those of the  $z$ -logistic map (namely,  $z_1 = z_2 = z$ ). Moreover, it is well known that this map family fails to exhibit the metric universality of Feigenbaum. In this case, the scaling factors (Feigenbaum numbers)  $\alpha_F$  and  $\delta$  present an oscillatory divergent behavior [24,25]. Same kind of oscillatory behavior has also been observed for multifractal function  $f(\alpha)$  [26].

Since  $q^*$  values were not available for asymmetric logistic map family, it was not possible to see the behavior of  $q^*$  as a function of the  $(z_1, z_2)$  pairs. On the other hand, in a very recent effort [7], in order to see this behavior, *without finding the precise values of  $q^*$  for  $(z_1, z_2)$  pairs*, one of us has used another technique based on the very recent generalization of bit cumulants for chaotic systems [27,28]. In spite of the fact that in  $q$ -generalized bit cumulant theory,  $q$  is a free parameter, it seems from the results of [7] that as  $z_2 - z_1 \rightarrow \pm \infty$ ,  $q^*$  will approach unity, which is similar to the behavior observed for symmetric maps studied so far [1–4].

We are now prepared to proceed with our numerical results for the asymmetric logistic map family. First of all, since our aim is to look at the properties of this family at the onset of chaos, the calculated values of the critical map parameter ( $a_c$ ) as a function of  $(z_1, z_2)$  pairs are given in Fig. 2 and in Table I. It is evident that the behavior of  $a_c$  values with respect to  $(z_2 - z_1)$  is very similar to the tendency of  $a_c$  values of the  $z$ -logistic family with respect to parameter  $z$ .

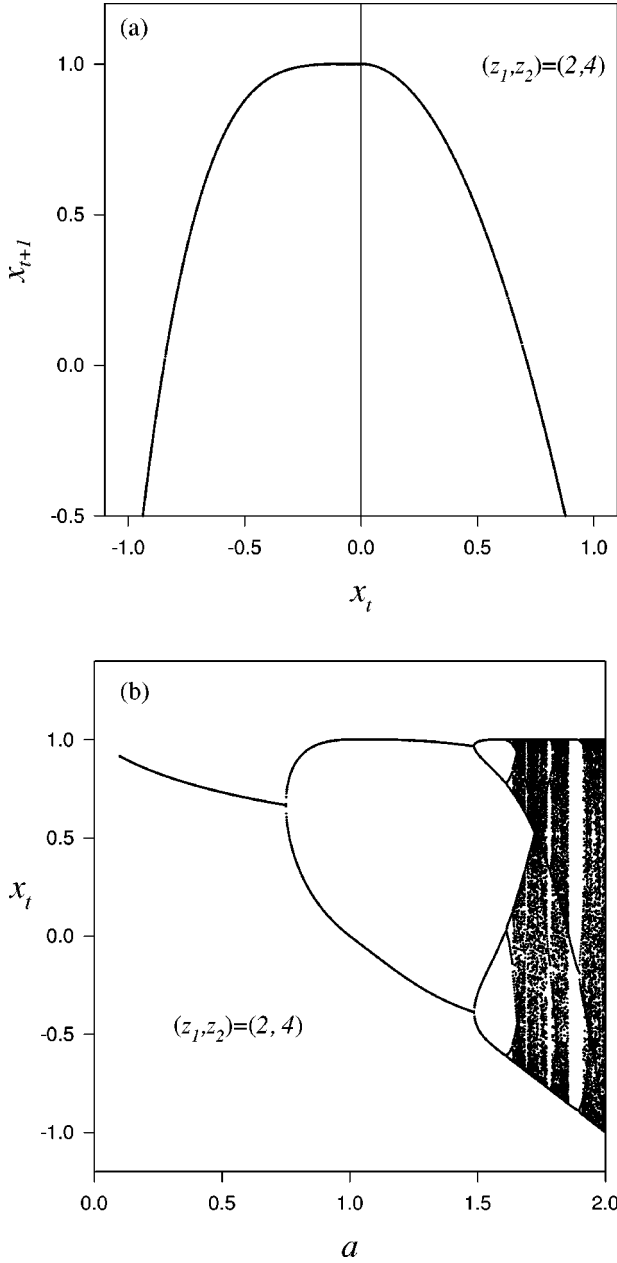


FIG. 1. (a) Asymmetric shape of the map given by Eq. (6) for the inflexion parameter pair (2, 4). (b) The bifurcation diagram of the map for the same inflexion parameter pair.

### A. First method

As already discussed above, this method is based on the sensitivity to initial conditions and for the asymmetric logistic map family, the sensitivity function  $\xi(t)$  is given by

$$\ln \xi(t) = \sum_{i=1}^t \ln \left[ \frac{df(x_i)}{dx} \right], \quad (7)$$

and exhibits, at the chaos threshold, a power-law divergence,  $\xi \propto t^{1/(1-q^*)}$ , from where  $q^*$  values can be calculated by measuring, on a log-log plot, the upper bound slope  $1/(1-q^*)$ . In Fig. 3, for  $x_0=0$ , the behavior of the sensitivity

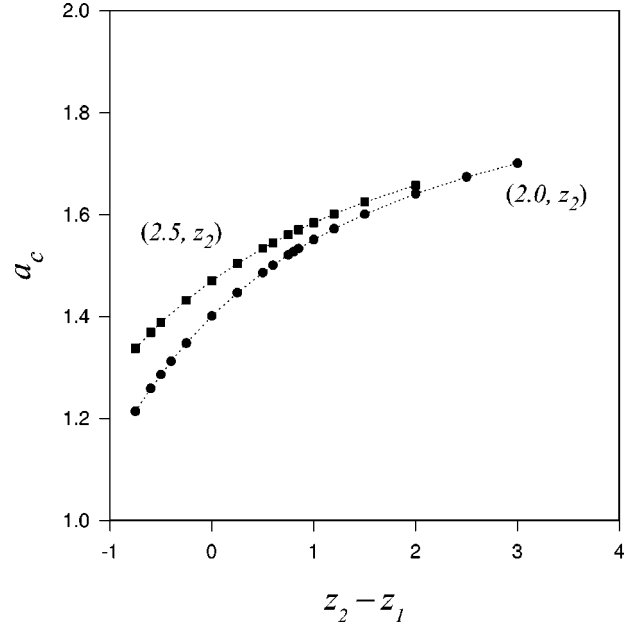


FIG. 2. The behavior of the critical map parameter  $a_c$  as a function of  $(z_2 - z_1)$  for two typical inflexion parameter pairs. The dotted lines are guides to the eye.

function [namely, the time evolution of Eq. (7)] has been illustrated for two typical  $(z_1, z_2)$  pairs. The slope of the upper bound has been calculated for each pair between the time interval [4, 8.5]. The calculation of the slope has been done by taking into account the points that lie on the upper bound within the above-mentioned time interval. We encountered that, as  $(z_2 - z_1)$  values become larger (that is the map becomes more asymmetric), the number of points that could be used in estimating the slope becomes fewer. For such

TABLE I. The values of  $a_c$  and  $q^*$  for various  $(z_1, z_2)$  pairs.

$(z_1, z_2)$	$a_c$	$q^*$
(2,1.25)	1.21403412 ...	$0.76 \pm 0.01$
(2,1.4)	1.25863959 ...	$0.62 \pm 0.01$
(2,1.5)	1.28613959 ...	$0.58 \pm 0.01$
(2,1.6)	1.31201155 ...	$0.49 \pm 0.01$
(2,1.75)	1.34799246 ...	$0.31 \pm 0.01$
(2,2)	1.40115518 ...	$0.24 \pm 0.01$
(2,2.25)	1.44691055 ...	$0.36 \pm 0.01$
(2,2.5)	1.48645043 ...	$0.47 \pm 0.01$
(2,2.75)	1.52083316 ...	$0.56 \pm 0.01$
(2,3)	1.55094551 ...	$0.63 \pm 0.01$
(2,3.5)	1.60109881 ...	$0.71 \pm 0.01$
(2.5,1.6)	1.30334301 ...	$0.72 \pm 0.01$
(2.5,1.75)	1.33742470 ...	$0.61 \pm 0.01$
(2.5,2)	1.38805851 ...	$0.49 \pm 0.01$
(2.5,2.5)	1.47055000 ...	$0.39 \pm 0.01$
(2.5,3)	1.53418776 ...	$0.49 \pm 0.01$
(2.5,3.25)	1.56070446 ...	$0.55 \pm 0.01$
(2.5,3.5)	1.58439440 ...	$0.60 \pm 0.01$
(2.5,4)	1.62488124 ...	$0.67 \pm 0.01$

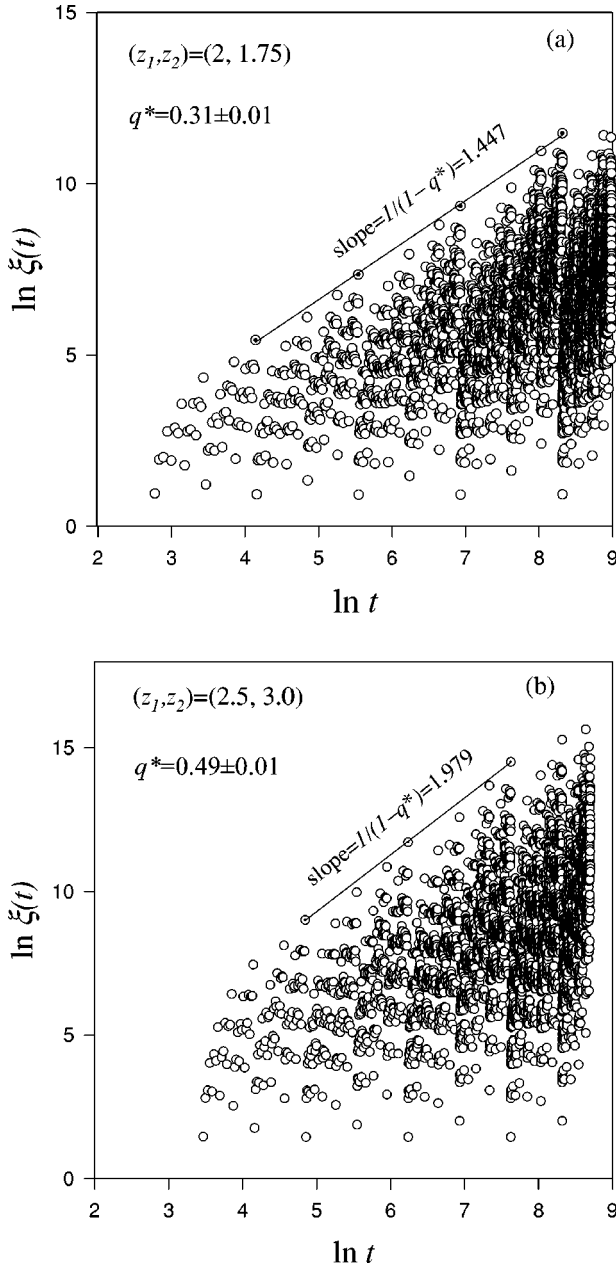


FIG. 3. Log-log plot of the sensitivity function versus time for (a) (2, 1.75) and (b) (2.5, 3) pairs.

cases, one should go for times larger than say 8.5 (in logarithmic scale), which requires much more precision on the values of  $a_c$ . On the other hand, for the  $(z_1, z_2)$  pairs given in the Table, the above mentioned time interval is good enough to determine the slope. From this slope, for each pair, we calculate the  $q^*$  values and in Fig. 4 we exhibit the behavior of  $q^*$  as a function of  $(z_2 - z_1)$  for two typical pairs. It is seen that as  $(z_2 - z_1)$  goes  $\pm\infty$ ,  $q^*$  becomes closer to unity without attaining it. This tendency is consistent with the recent claim of Ref. [7] and also similar to the behavior of symmetric map families studied so far [1–4,29].

### B. Second method

As mentioned previously, for this asymmetric family, the multifractal function  $f(\alpha)$  fluctuates considerably for differ-

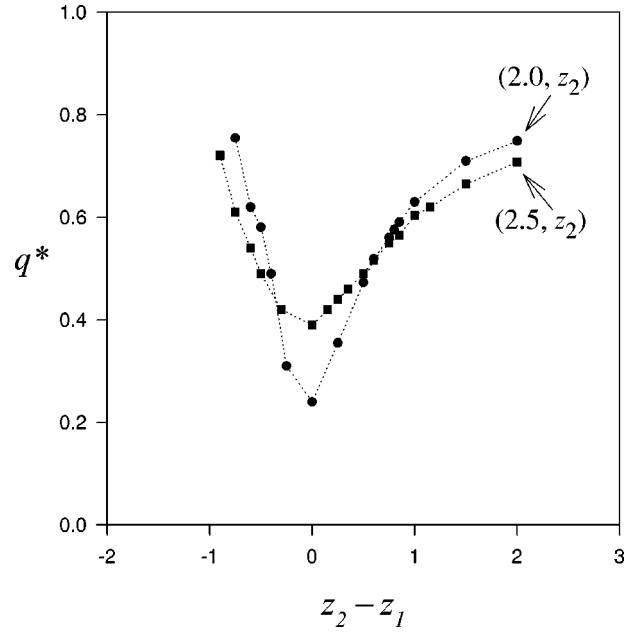


FIG. 4. The behavior of  $q^*$  values as a function of  $(z_2 - z_1)$  for  $(2, z_2)$  and  $(2.5, z_2)$ . The dotted lines are guides to the eye. See the Table for typical error bars.

ent number of iterations ( $I$ ) that prevents us from estimating the exact values of  $\alpha_{min}$  and  $\alpha_{max}$  from where we determine  $q^*$  values. Worse than that, this problem cannot be cured by extrapolating the number of iterations to infinity as it is done in Ref. [4] for the  $z$ -circular maps and [9] for the single-site map. In  $z$ -circular case, the fluctuations are so systematic that one can extrapolate the results to infinite number of iterations with acceptable precision from where  $\alpha_{min}$  and  $\alpha_{max}$  values could be deduced, whereas for asymmetric logistic family this is not the case. To illustrate this, we plotted the  $f(\alpha)$  curve for the inflexion pair (2,3) in Fig. 5(a), where the oscillatory behavior is evident. Moreover, we presented in Fig. 5(b), the extrapolation of  $\alpha_{min}$  and  $\alpha_{max}$  for the same pair. It is clear from the confidence interval that it is not possible to estimate their correct values due to large fluctuations. This yields us to conclude that for this asymmetric map family, the second method cannot be used easily to determine  $q^*$  values due to the unavoidable fluctuations in the  $f(\alpha)$  function. In fact, this result has also been supported by a recent observation: One of us has shown recently [29] that for  $z$ -logistic maps, the scaling relation given in Eq. (3) can be reexpressed as  $1/(1-q) = [(z-1)\ln 2]/[\ln \alpha_F(z)]$ , which clearly points out that this scaling is dependent on Feigenbaum constant  $\alpha_F$ . Since for the asymmetric map family we are studying, as already mentioned, the Feigenbaum numbers exhibit oscillatory divergent behavior [24,25], it is evident that  $q^*$  values cannot be easily and reliably inferred from the scaling relation due to these fluctuations.

### C. Third method

Finally, in order to verify the results of the first method, let us use the entropy increase rate procedure to estimate the proper  $q^*$  values. The procedure is the following: First, we

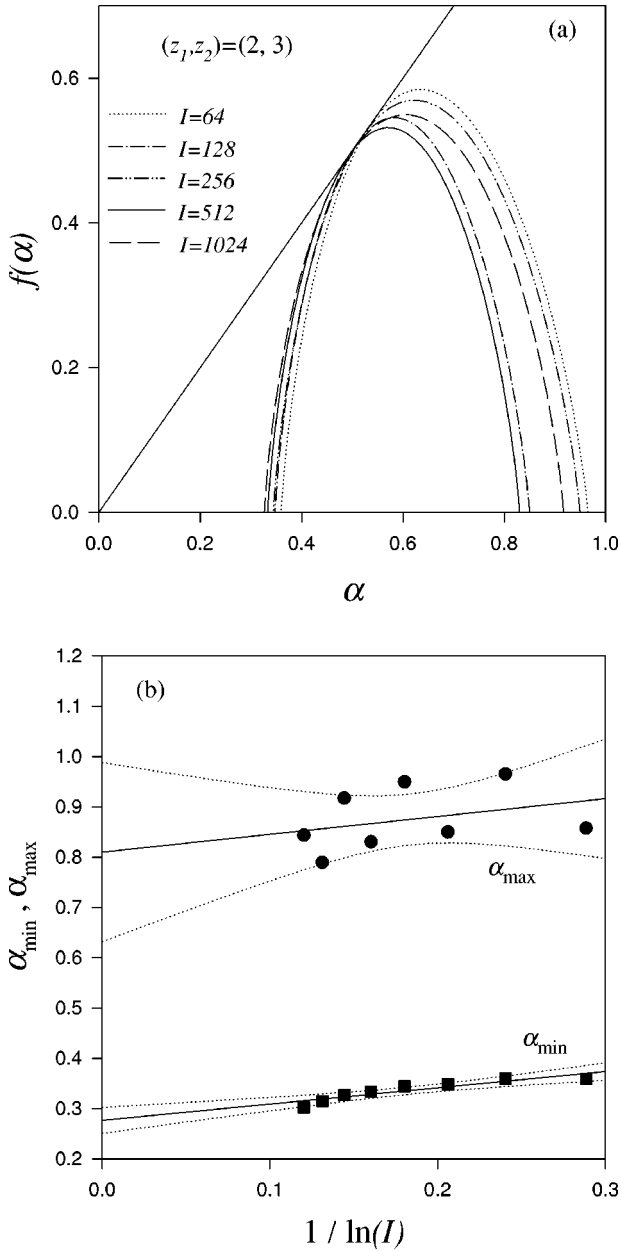


FIG. 5. (a) The behavior of  $f(\alpha)$  curve for various values of the number of iterations. (b) The oscillatory behavior of  $\alpha_{\min}$  and  $\alpha_{\max}$ . The dotted lines are standard confidence intervals (SigmaPlot 1.00).

partition the phase space into  $W$  equal cells, then we choose one of them and select  $N$  initial conditions (all inside the chosen cell). As  $t$  evolves, these initial conditions spread within the phase space and naturally this gives us a set  $\{N_i(t)\}$  with  $\sum_{i=1}^W N_i(t) = N, \forall t$ , which consequently yields a set of probabilities  $\{p_i(t) \equiv N_i(t)/N\}$ . At the beginning of time, clearly  $S_q(0) = 0$ , then it gradually exhibits three successive regions as first indicated in Ref. [30] for a different system. In the first region, the entropy is roughly constant in time, then it starts increasing in the second region and finally it tends towards its saturation value. This indicates that the linear increase of the proper entropy is expected to emerge in the second (intermediate) region. As clearly explained in

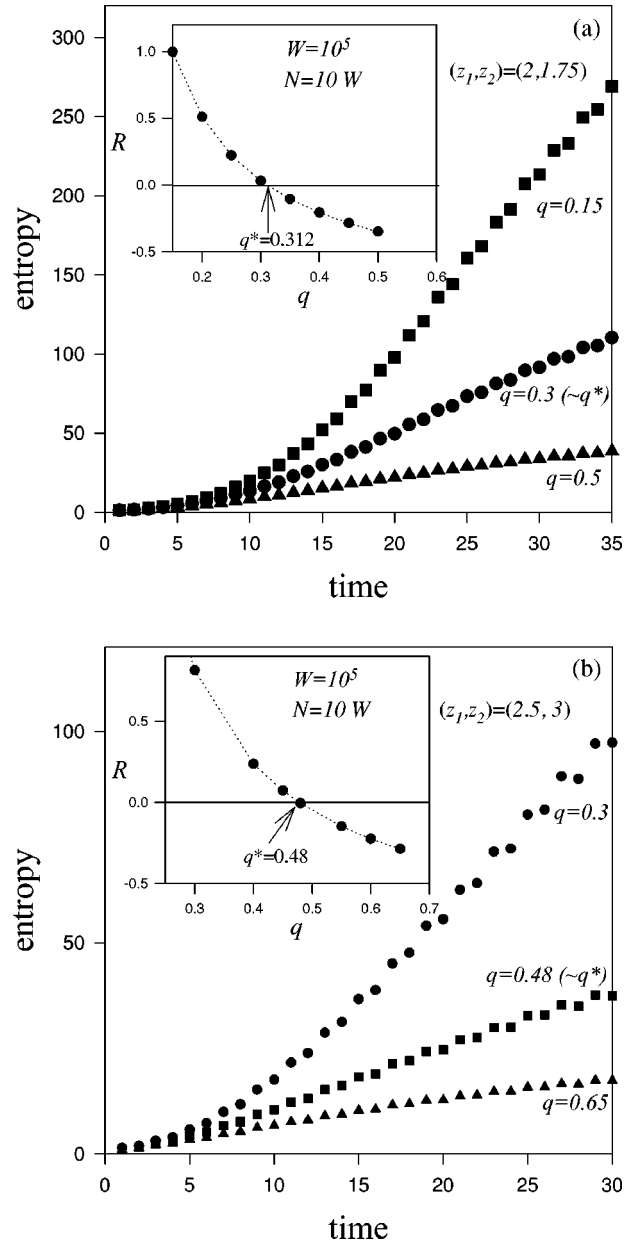


FIG. 6. Time evolution of the entropy for three different values of  $q$  for (a) (2, 1.75); (b) (2.5, 3) pairs. Insets: The nonlinearity coefficient  $R$  versus  $q$ . The interval characterizing the intermediate region is [13,31] for (a) and [7,25] for (b). The dotted lines are guides to the eye.

Refs. [5,6], at the chaos threshold, very large fluctuations appear in the entropy due to the fact that the critical attractor occupies only a tiny part of the available phase space. To overcome this problem, we use a procedure of averaging over the efficient initial conditions as discussed in Refs. [5,6]. Since this procedure is very time-consuming, we apply it for two typical  $(z_1, z_2)$  pairs to check the results of the first method. The results are given in Fig. 6. It is observed that, for all cases, in the intermediate region, the linear increase of the entropy with time emerges only for a special value of  $q$  (namely,  $q^*$ ), and this value corresponds, within a good precision, to the one obtained from the first method. On the

other hand, for  $q < q^*$  ( $q > q^*$ ) it curves upwards (downwards). To provide quantitative support to this, we fit the curves with the polynomial  $S_q(t) = A + Bt + Ct^2$  in the interval  $[t_1, t_2]$  characterizing the intermediate region. The nonlinearity coefficient  $R \equiv C(t_1 + t_2)/B$  is a measure of the importance of the nonlinear term, therefore,  $R$  vanishes for a strictly linear fit. These results are given as insets of Fig. 6.

### III. CONCLUSIONS

In this work, we performed an extensive analysis of the sensitivity to initial conditions problem related to a family of asymmetric maps at the edge of chaos. We have been particularly interested in exploiting the connections between the sensitivity function, generalized nonextensive entropies and the multifractal character of the critical attractor.

A direct numerical computation of the sensitivity function  $\xi(t)$ , which measures the temporal evolution of the distance between initially nearby trajectories, shows strong fluctuations whose upper bounds delimit a power-law growth  $\xi(t) \propto t^{1/(1-q^*)}$ . The characteristic power-law exponent was determined for several pairs of the inflexions at the left and right of map inflexion point. For extremely asymmetric maps, wild fluctuations do not allow the power-law exponents to be determined with high accuracy, but the general trend indicates that  $q^*$  approaches unity in the limit of very asymmetric maps.

We also employed a multifractal analysis, based on the standard Halsey *et al.* algorithm [13], to compute the singularity spectrum  $f(\alpha)$  related to the critical attractor of the present family of asymmetric maps. A recently proposed scaling relation associates the extremal points of the  $f(\alpha)$

curve with the power-law exponent governing the sensitivity function. However, the numerical method used to compute  $f(\alpha)$  exhibits large fluctuations when applied to these asymmetric maps due to the divergent oscillatory behavior of the Feigenbaum numbers. This feature makes the precise estimation of the location of its extremal points difficult. It would be valuable to have an alternative algorithm to compute the  $f(\alpha)$  curve that could overcome this point to allow a fine check of the accuracy of the scaling relation [Eq. (3)] for these asymmetric maps.

Finally, the sensitivity to initial conditions was investigated by computing the rate of increase of generalized entropies  $S_q$ . At the edge of chaos, there is a particular entropic index  $q^*$  for which the entropy grows, in the infinitely fine-graining limit, at a stationary rate after a short initial transient. This method provides values for  $q^*$  that are in agreement with the ones obtained from the direct measure of the sensitivity function. Although being more time consuming, the entropy measure is free from wild fluctuations and allows for a relatively fine and confident estimate of  $q^*$ . Therefore, this method should be the starting point to investigate the possibility of similar power-law sensitivity to initial conditions in higher dimensional as well as conservative nonlinear dynamical systems (see, for instance, Ref. [31]).

### ACKNOWLEDGMENTS

One of us (U.T.) acknowledges partial support from the Ege University Research Fund under Project No. 2000FEN049. This work was also partially supported by PRONEX, CNPq, CAPES, FAPEAL, and FAPERJ (Brazilian agencies).

- 
- [1] C. Tsallis, A. R. Plastino, and W.-M. Zheng, *Chaos, Solitons Fractals* **8**, 885 (1997).
  - [2] U. M. S. Costa, M. L. Lyra, A. R. Plastino, and C. Tsallis, *Phys. Rev. E* **56**, 245 (1997).
  - [3] M. L. Lyra and C. Tsallis, *Phys. Rev. Lett.* **80**, 53 (1998).
  - [4] U. Tirnakli, C. Tsallis, and M. L. Lyra, *Eur. Phys. J. B* **11**, 309 (1999).
  - [5] V. Latora, M. Baranger, A. Rapisarda, and C. Tsallis, *Phys. Lett. A* **273**, 97 (2000).
  - [6] U. Tirnakli, G. F. J. Ananos, and C. Tsallis, *Phys. Lett. A* **289**, 51 (2001).
  - [7] U. Tirnakli, *Phys. Rev. E* **62**, 7857 (2000).
  - [8] C. R. da Silva, H. R. da Cruz, and M. L. Lyra, *Braz. J. Phys.* **29**, 144 (1999).
  - [9] U. Tirnakli, *Physica A* (to be published) (e-print cond-mat/0109278).
  - [10] P. Grassberger and M. Scheunert, *J. Stat. Phys.* **26**, 697 (1981).
  - [11] T. Schneider, A. Politi, and D. Wurtz, *Z. Phys. B: Condens. Matter* **66**, 469 (1987); G. Anania and A. Politi, *Europhys. Lett.* **7**, 119 (1988).
  - [12] H. Hata, T. Horita, and H. Mori, *Prog. Theor. Phys.* **82**, 897 (1989).
  - [13] T. C. Halsey *et al.*, *Phys. Rev. A* **33**, 1141 (1986).
  - [14] C. Beck and F. Schlogl, *Thermodynamics of Chaotic Systems* (Cambridge University Press, Cambridge, 1993).
  - [15] R. C. Hilborn, *Chaos and Nonlinear Dynamics* (Oxford University Press, New York, 1994).
  - [16] S. Montangero, L. Fronzoni, and P. Grigolini, *Phys. Lett. A* **285**, 81 (2001).
  - [17] C. Tsallis, *J. Stat. Phys.* **52**, 479 (1988).
  - [18] E. M. F. Curado and C. Tsallis, *J. Phys. A* **24**, L69 (1991); **24**, 3187(E) (1991); **25**, 1019(E) (1992); C. Tsallis, R. S. Mendes, and A. R. Plastino, *Physica A* **261**, 534 (1998).
  - [19] A set of mini reviews is available in C. Tsallis, *Braz. J. Phys.* **29**, 1 (1999); in *Nonextensive Statistical Mechanics and its Applications*, edited by S. Abe and Y. Okamoto, Lecture Notes in Physics (Springer, Berlin, 2001).
  - [20] I. Bediaga, E. M. F. Curado, and J. Miranda, *Physica A* **286**, 156 (2000).
  - [21] C. Beck, G. S. Lewis, and H. L. Swinney, *Phys. Rev. E* **63**, 035303 (2001); T. Arimitsu and N. Arimitsu, *J. Phys. A* **33**, L235 (2000); **34**, 673(E) (2001).
  - [22] A. Upadhyaya, J.-P. Rieu, J. A. Glazier, and Y. Sawada, *Physica A* **293**, 549 (2001).
  - [23] F. A. B. F. de Moura, U. Tirnakli, and M. L. Lyra, *Phys. Rev. E* **62**, 6361 (2000).

- [24] R. V. Jensen and L. K. H. Ma, Phys. Rev. A **31**, 3993 (1985).
- [25] M. C. de Sousa Vieira, E. Lazo, and C. Tsallis, Phys. Rev. A **35**, 945 (1987).
- [26] M. C. de Sousa Vieira and C. Tsallis, Phys. Rev. A **40**, 5305 (1989).
- [27] R. S. Johal and R. Rai, Physica A **282**, 525 (2000).
- [28] R. Rai and R. S. Johal, Physica A **294**, 155 (2001).
- [29] M. L. Lyra, Annu. Rev. Comput. Phys. **6**, 31 (1999).
- [30] V. Latora and M. Baranger, Phys. Rev. Lett. **82**, 520 (1999).
- [31] F. Baldovin, C. Tsallis, and B. Schulze, e-print cond-mat/0108501.